AIP | Applied Physics Letters

Correlation between Ti source/drain contact and performance of InGaZnO-based thin film transistors

Kwang-Hyuk Choi and Han-Ki Kim

Citation: Appl. Phys. Lett. **102**, 052103 (2013); doi: 10.1063/1.4790357
View online: http://dx.doi.org/10.1063/1.4790357
View Table of Contents: http://apl.aip.org/resource/1/APPLAB/v102/i5
Published by the American Institute of Physics.

Correlation between Ti source/drain contact and performance of InGaZnO-based thin film transistors

Kwang-Hyuk Choi and Han-Ki Kim[a)]
Department of Advanced Materials Engineering for Information and Electronics, Kyung Hee University, 1 Seocheon-dong, Yongin-si, Gyeonggi-do 446-701, South Korea

(Received 21 September 2012; accepted 14 January 2013; published online 4 February 2013)

Ti contact properties and their electrical contribution to an amorphous InGaZnO (*a*-IGZO) semiconductor-based thin film transistor (TFT) were investigated in terms of chemical, structural, and electrical considerations. TFT device parameters were quantitatively studied by a transmission line method. By comparing various *a*-IGZO TFT parameters with those of different Ag and Ti source/drain electrodes, Ti S/D contact with an *a*-IGZO channel was found to lead to a negative shift in V_T ($-\Delta$ 0.52 V). This resulted in higher saturation mobility (8.48 cm^2/Vs) of *a*-IGZO TFTs due to effective interfacial reaction between Ti and an *a*-IGZO semiconducting layer. Based on transmission electron microcopy, x-ray photoelectron depth profile analyses, and numerical calculation of TFT parameters, we suggest a possible Ti contact mechanism on semiconducting *a*-IGZO channel layers for TFTs. © *2013 American Institute of Physics*. [http://dx.doi.org/10.1063/1.4790357]

During the last few decades, amorphous indium-gallium-zinc-oxide (*a*-IGZO) semiconductor-based thin film transistors (TFTs) have gained attention as candidates to substitute for conventional amorphous Si:H TFTs in active matrix liquid crystal displays and organic light emitting diodes. The *a*-IGZO TFTs are excellent performers and allow low temperature processes.[1–3] Proper selection of source and drain (S/D) contact materials is very important for high performance *a*-IGZO TFTs because gate bias-induced current values, field effect mobility, and switching properties are critically affected by the contact properties of S/D electrodes.[4–7] For this reason, titanium (Ti) and molybdenum (Mo) have been widely employed in academic and industry research groups as S/D electrodes for *a*-IGZO TFTs.[8,9] Considering the work function of *a*-IGZO (~4.5 eV), Ti (4.3 eV), and Mo (4.7 eV) metals are quite reasonable as S/D electrodes. Ti or Mo contact on *a*-IGZO leads to a negligible Schottky barrier height between S/D electrodes and the *a*-IGZO semiconducting layer.[10] Kim *et al.* recently reported the carrier transport mechanism of Ti contact with *a*-IGZO in terms of specific contact resistivity.[11] They reported that Ti contact on conductive IGZO layers with high carrier concentration (1.3×10^{19} cm^{-3}) produced high performance Ohmic contact with a specific contact resistivity as low as 2.85×10^{-5} $\Omega\,cm^2$. Although they suggested a possible Ti ohmic contact mechanism, some issues related to the effects of Ti/*a*-IGZO on *a*-IGZO TFT device performance still remain. In normal n-type *a*-IGZO TFT devices that operate with on voltage (V_{ON}) around $V_{GS} = 0$ V and on-to-off current ratio ($I_{on/off}$) of ~10^{10}, the carrier concentration of *a*-IGZO semiconducting layers is not as high as >~10^{19} cm^{-3} (generally ~10^{17} cm^{-3}).[1] With those semiconducting layers, the *a*-IGZO TFTs cannot operate in normal switching operations due to high off current values.[12] For comparison, current-voltage curves with a normal *a*-IGZO semiconducting layer used in practical TFT devices are shown in Fig. 1(a). It is imperative to investigate the Ti metal contact properties between Ti metal and *a*-IGZO semiconducting layers and their influence on TFT device performance as S/D electrodes.

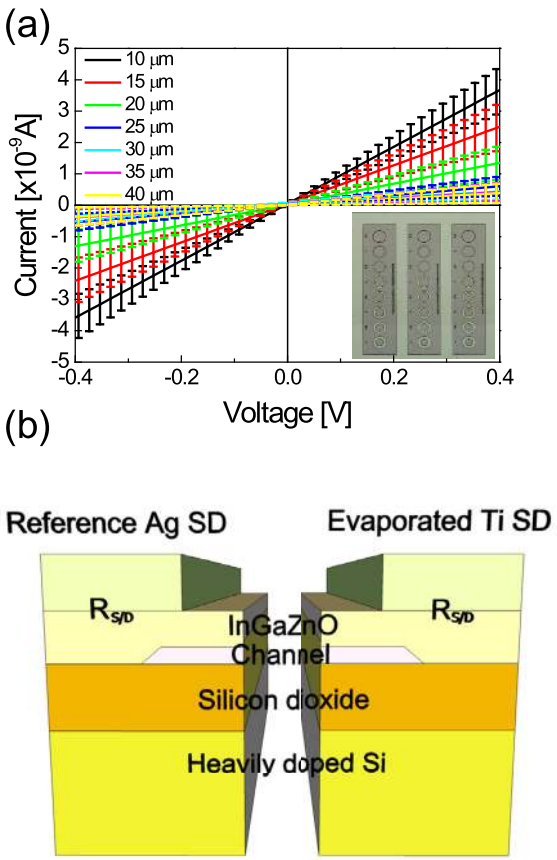

FIG. 1. (a) I-V curves resulting from a 50-nm-thick *a*-IGZO-based semiconducting layer with Ti contacts as a function of different Ti pad spacing (10, 15, 20, 25, 30, 35, and 40 μm), calculated by circular transmission length method. A 50-nm-thick *a*-IGZO-based semiconducting layer was prepared through an identical TFT process. (b) Cross sectional illustration of *a*-IGZO TFT with bottom gate and top contact structure.

[a)]Author to whom correspondence should be addressed. Electronic mail: imdlhkkim@khu.ac.kr.

In this letter, we concatenate Ti metal contact properties with their electrical contribution in low carrier concentration *a*-IGZO semiconductor-based TFTs. TFT device parameters, such as field-effect mobility at saturation region (μ_{SAT}), subthreshold swing (SS), threshold voltage (V_T), and effective contact resistivity (r_{Ceff}), were quantitatively studied. By comparing TFT parameters of *a*-IGZO TFTs with different Ag and Ti S/D electrodes, we found that IGZO TFT performance was closely related to lower resistance metal contact. This influenced lower r_{Ceff} and $R_{S/D}$ values in the vicinity of S/D electrodes. Based on transmission electron microcopy (TEM), x-ray photoelectron (XPS) depth profile analysis, and numerical calculations of TFT parameters, a possible Ti contact mechanism for TFTs on semiconducting IGZO channel layers was suggested.

a-IGZO TFTs with conventional bottom-gate and top S/D contact structures were fabricated. As shown in Fig. 1(b), an *a*-IGZO layer was thoroughly coated onto the SiO_2 dielectric layer to avoid gate over-rapping dependent series resistance behavior. Heavily doped Si ($\sim 10^{-4}$ Ω cm) and thermal-grown 100-nm-thick SiO_2 were used as the gate electrode and dielectric layer. A 50-nm-thick *a*-IGZO semiconducting layer was deposited by a conventional radio-frequency (RF) magnetron sputtering system using IGZO (In_2O_3:ZnO:Ga_2O_3 = 1:1:1 mol) target material at a constant RF power density of 2.2 W/cm^2, working pressure of 2 mTorr, and O_2/Ar gas flow ratio of 0.015. After deposition, *a*-IGZO semiconducting layers were thermally annealed at 300 °C for 1 h under atmospheric ambient. Then, 50-nm-thick Ti S/D electrodes were deposited by thermal evaporation and patterned by a conventional photolithographic lift-off method. To compare S/D contact effects on the electrical contribution in TFT devices, highly conductive (4.72×10^{-6} Ω cm) 50 nm thick reference Ag S/D electrodes were employed with the same evaporation apparatus. During sputtering and thermal evaporation, the substrate temperature was held at less than 50 °C. The resistivity of Ti and Ag metal S/D was measured by Hall measurement equipment with van der Pauw configuration (HL5500PC, Accent Optical Technology). The S/D series resistance ($R_{S/D}$), effective contact resistivity (r_{Ceff}), and effective transfer length (L_T) of *a*-IGZO TFTs were confirmed by a well-known transmission line method (TLM) that uses photolithographic lift-off patterning. All device characterizations in this experiment were analyzed by a customized probe station (HP4145B) system in a light tight box. Structural and chemical properties were characterized by high-resolution transmission electron microscopy (HRTEM: JEOL JEM2100F) and X-ray photoelectron spectroscopy (XPS: Thermo Scientific) depth profiles, respectively.

XPS depth profile and HRTEM examinations were performed to correlate the electrical and interfacial reactions between Ti and *a*-IGZO. Figure 2(a) shows core O1*s* and Ti2*p* level spectra of XPS depth profiles obtained from the Ti/*a*-IGZO interface and *a*-IGZO semiconducting layer regions in TFT devices. Unlike with *a*-IGZO semiconducting regions, core O1s level spectra in the vicinity of the Ti/*a*-IGZO interface exhibited additional binding energies of 531.56 eV corresponding to oxygen vacancy states. This additional binding energy indicates oxygen deficient states of *a*-IGZO at the region of interfaces.[13] In general, oxygen vacancies in the IGZO matrix act as donors, so the formation of oxygen

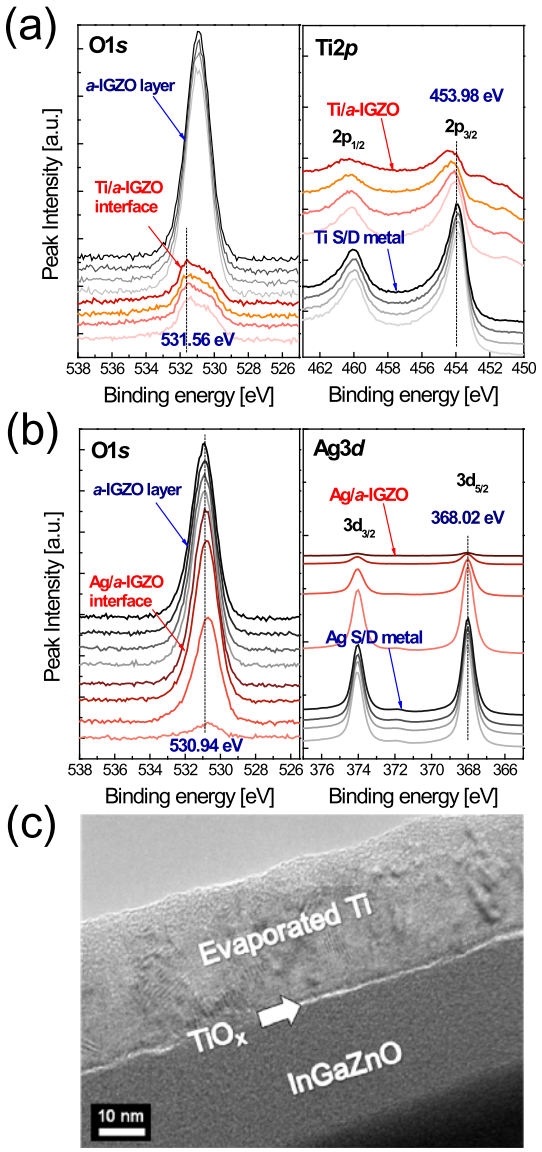

FIG. 2. Core O1s, Ti2*p*, and Ag3*d* level spectra obtained from (a) Ti/*a*-IGZO and (b) Ag/a-IGZO interfaces from the TFT devices. (c) Cross sectional HRTEM image of *a*-IGZO TFT with Ti S/D electrode showing thin interfacial TiO_x layer.

deficient IGZO regions could increase carrier concentration. The core Ti2*p* level spectra obtained from the Ti S/D and Ti/*a*-IGZO interface regions also showed different chemical states. The Ti 2*p* core level peak obtained from the Ti electrode layer showed a binding energy of 453.98 eV, which indicated a complete Ti metal layer.[14] However, the Ti 2*p* core level peak at the Ti/*a*-IGZO interface showed multiplicity of intermediate Ti oxidation states (TiO_x). These phenomena in chemical shifts at the Ti/*a*-IGZO interfacial region were entirely different from the chemical states at the Ag/*a*-IGZO region. As shown in Fig. 2(b), any chemical shifts at the vicinity of Ag/*a*-IGZO interface were observed after evaporation of Ag S/D contacts indicating that there is no oxygen vacancies generation by Ag S/D contact. As expected from the XPS profiles in Fig. 2(a), the cross-sectional HRTEM image clearly demonstrated the existence of a very thin TiO_x interfacial layer between Ti S/D and *a*-IGZO semiconducting layers in Fig. 2(c). Rough interface and bright contrast at the interface implies that an interfacial reaction occurred during a Ti metal evaporation

process. The formation of interfacial TiO_x layers can be explained by formation enthalpies (ΔH_{TiOx}), as previously reported for Ti/AlZnO contact.[15] Because the formation enthalpies of Ti_2O_3 ($\Delta H_{Ti2O3} = -1520.9$ kJ/mol), Ti_2O_5 ($\Delta H_{Ti2O5} = -2046.0$ kJ/mol), Ti_3O_5 ($\Delta H_{Ti3O5} = -2459.4$ kJ/mol), and TiO_2 ($\Delta H_{TiO2} = -944.0$ kJ/mol) are much lower than those of In_2O_3 ($\Delta H_{In2O3} = -925.8$ kJ/mol), Ga_2O ($\Delta H_{Ga2O} = -3565.0$ kJ/mol), Ga_2O_3 ($\Delta H_{TiO2} = -1089.1$ kJ/mol), and ZnO ($\Delta H_{ZnO} = -350.5$ kJ/mol), the formation of TiO_x at the interfacial region between Ti and IGZO layers by oxygen out-diffusion from IGZO is reasonable. Kim *et al.* proposed a similar Ti/IGZO mechanism based on formation enthalpy. They explained that the lower TiO_x enthalpy values could result in significant out-diffusion of In, Ga, and Zn at the Ti/IGZO contact region.[11]

Figures 3(a) and 3(b) show electrical transfer curves of *a*-IGZO TFTs with reference Ag and Ti S/D electrodes

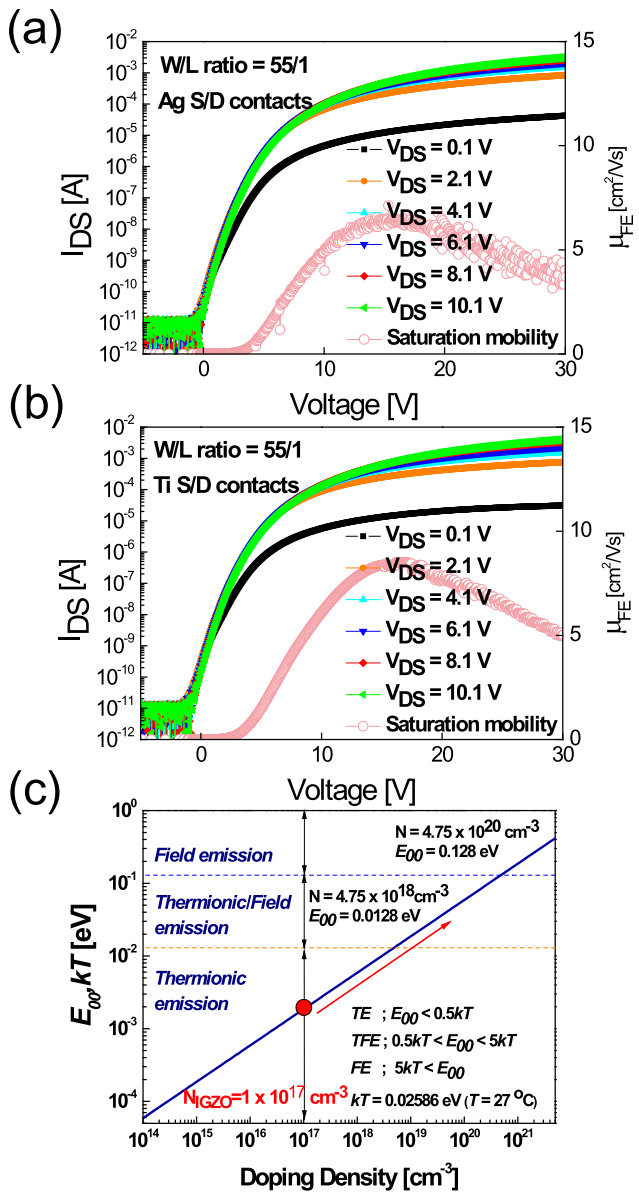

FIG. 3. Transfer characteristics of *a*-IGZO-based thin film transistors with evaporation-deposited (a) Ag and (d) Ti S/D electrodes. Saturation mobility (μ_{SAT}) values were obtained at V_{DS} of 10.1 V. (c) E_{00} and kT as functions of doping density of *a*-IGZO semiconducting layer.

without a post-annealing process after S/D deposition. To identify the electrical contribution of Ti contact in the devices, Ag and Ti S/D electrodes were prepared on identical *a*-IGZO semiconducting layers. Field effect mobility at the saturation region (μ_{SAT}) and SS values were extracted from transfer curves by the following equations:[16]

$$I_{DS} = \frac{C_{OX}\mu_{sat}W}{2L}(V_{GS} - V_T)^2, (V_{DS} = 10.1\,V) \quad (1)$$

and

$$SS = \frac{\partial V_{GS}}{\partial(\log I_{DS})}, \quad (2)$$

where I_{DS} is drain current, C_{ox} is capacitance per unit area, V_{GS} is gate voltage, and V_T is the threshold voltage that induced a current value of W/L × nA at 10.1 V_{DS}. The detailed performance of TFTs for both S/D electrodes is summarized in Table I. The transfer curves of TFTs with Ti S/D electrodes exhibited similar behavior to those of TFTs with Ag S/D electrodes even though Ti S/D has a fairly high electrical resistivity (1.66×10^{-4} Ω cm) compared to Ag S/D (4.72×10^{-6} Ω cm). The $I_{on/off}$ values of *a*-IGZO with Ag and Ti S/D electrodes were found to be 4.54×10^{10} and 4.66×10^{10}, respectively. However, the *a*-IGZO TFT with Ti S/D exhibited a slightly negative shifted V_T (−Δ 0.52 V) value compared to that of the TFT with Ag S/D electrodes (3.98 V). In general, negative V_T shifts for n-type TFTs are believed to be associated with the relatively large carrier concentration of *a*-IGZO.[10] In this experiment, *a*-IGZO layer thickness and process conditions were identically confined. Therefore, the negative shift in V_T can be interpreted as an increased carrier concentration in the *a*-IGZO semiconducting layer that resulted due to TiO_x formation at the interface. In addition, the *a*-IGZO TFT with Ti S/D showed a higher μ_{SAT} value (8.48 cm^2/Vs) than the *a*-IGZO TFT with Ag S/D electrodes (7.12 cm^2/Vs). Lee *et al.* recently reported that thermionic/field emission current is dominant under large V_{DS} bias conditions ($V_{DS} > 10.1$ V in our device).[18] With our *a*-IGZO semiconducting layer, carrier concentration was found to be approximately $6 \times 10^{16}\,cm^{-3}$–$1 \times 10^{17}\,cm^{-3}$. Assuming that the carrier concentration of the *a*-IGZO semiconducting layer is around $\sim 10^{17}\,cm^{-3}$, current flow at V_{DS} around 10.1 V should be governed by thermionic emission rather than thermionic/field emission, as shown in Fig. 3(c). Therefore, this enhanced

TABLE I. Comparative table of device performance for amorphous IGZO TFTs with Ag (4.72×10^{-6} Ω cm) and Ti (1.66×10^{-4} Ω cm) source/drain electrodes including saturation mobility (μ_{SAT}), SS, off current value (I_{off}), on current value (I_{on}), and on-to-off current ratio ($I_{on/off}$), respectively.

S/D materials	Ag	Ti
ρ (Ω cm)	4.72×10^{-6}	1.66×10^{-4}
μ_{SAT} (cm^2/Vs)	7.12	8.48
SS (V/decade)	0.88	0.87
I_{off} (A)	1.50×10^{-13}	1.46×10^{-13}
I_{on} (A)	6.81×10^{-3}	6.82×10^{-3}
I_{on}/I_{off}	4.54×10^{10}	4.66×10^{10}
V_T (V)	3.98	3.46

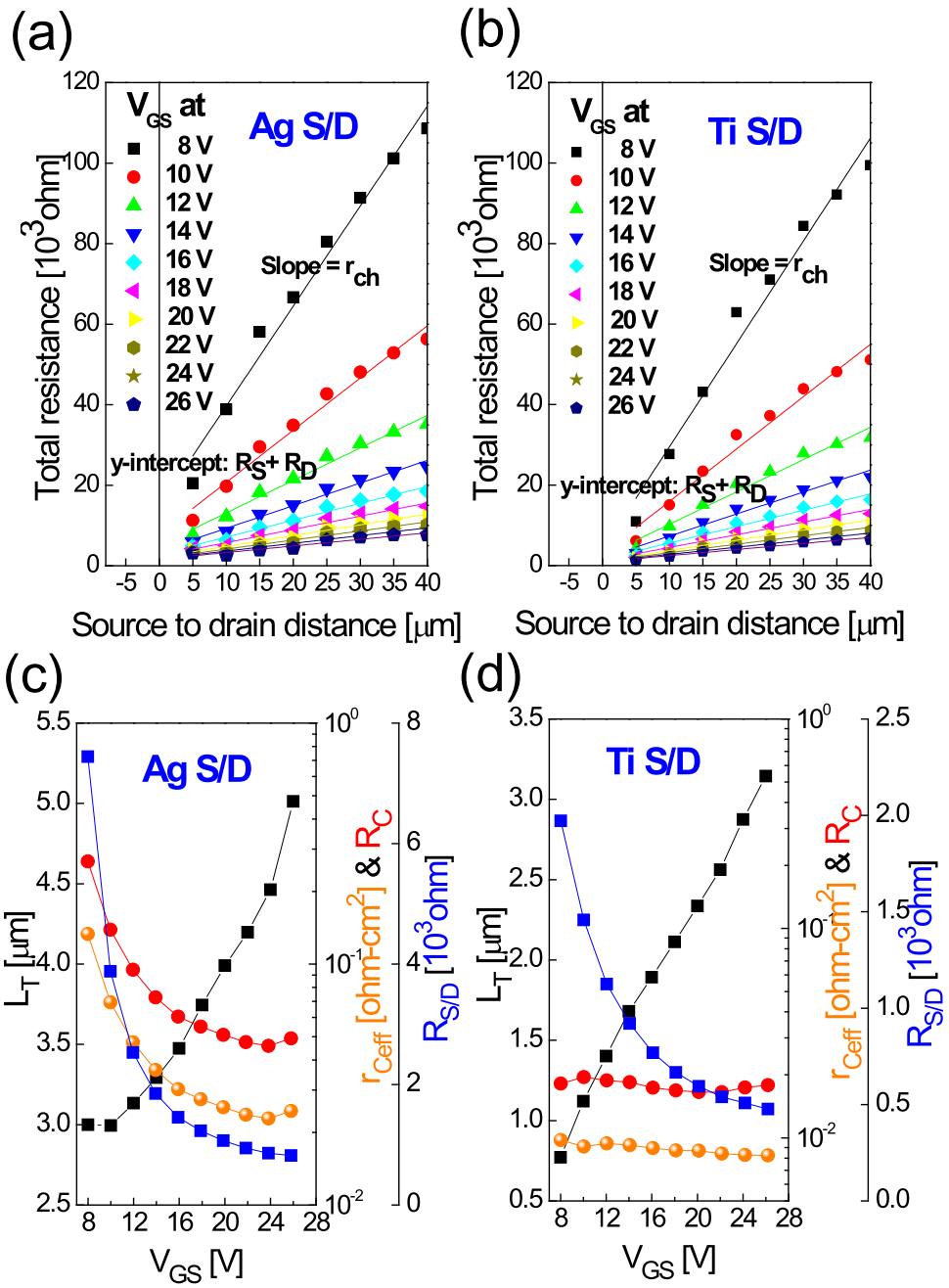

FIG. 4. Total ON resistance (R_T) plotted with respect to *a*-IGZO TFT channel length for different V_{GS} with (a) reference Ag and (c) Ti S/D electrodes in TFTs (symbol: measured data, lines: fitted lines). Evolution of effective channel length (L_T), effective contact resistivity (r_{Ceff}), and S/D series resistances ($R_{S/D}$) as functions of V_{GS} for *a*-IGZO TFTs with (b) Ag and (d) Ti S/D electrodes.

μ_{SAT} value at large V_{DS} (around 10.1 V) could be interpreted due to the influence of Ti and IGZO interfacial reaction on thermionic/filed emission enhancement. The current flow mechanism between metals and semiconductors was determined by characteristic energy E_{00}, defined as[19]

$$E_{00} = \frac{qh}{4\pi}\sqrt{\frac{N}{K_s\varepsilon_0 m^*_{tun}}} = 1.86\times10^{-11}\sqrt{\frac{N(cm^{-3})}{K_s(m^*_{tun}/m)}}[\mathrm{eV}], \tag{3}$$

where q is electron charge, h is Planck's constant (6.626×10^{-34} J·s), N is doping density, K_s is the dielectric constant of *a*-IGZO semiconductors (10.2), m_{tun} is the tunneling effective mass and m is electron mass. The formation of TiO_x interfacial layers retains oxygen vacancies at the surface of the *a*-IGZO channel layer. Because of this, the carrier concentration of *a*-IGZO channel layers could increase after interfacial reactions. We believe that the E_{00} value increased for this interfacial layer and the current flow mechanism changed from thermionic to thermionic/field emission.

To quantitatively investigate the effects of Ti S/D contact on TFT device parameters, source and drain series resistance ($R_{S/D}$), effective contact resistivity (r_{Ceff}), and effective transfer length (L_T) were calculated by the TLM.[16] Different TFT channel lengths were set at 5, 10, 15, 20, 25, 30, 35, and 40 μm. A global gate electrode was used to minimize the gate dependent $R_{S/D}$ behavior because small gate overlap to source (or drain) electrode can cause large $R_{S/D}$. Figures 4(a) and 4(b) show total TFT ON resistance (R_T) for both *a*-IGZO TFTs with respect to TFT channel length for different V_{GS}. Figures 4(c) and 4(d) exhibit V_{GS} dependent electrical parameters of *a*-IGZO TFT with reference Ag and Ti S/D electrodes. R_T is expressed by following equation:[16]

$$R_T = \frac{V_{DS}}{I_{DS}} = r_{ch}L + 2R_{S/D}, \quad (4)$$

where $2R_{S/D}$ is total (source + drain) series resistance and r_{ch} is channel resistance per channel length, which is defined by slope in R_T versus source-to-drain distance. The L_T, r_{Ceff}, and contact resistivity (R_C) values for *a*-IGZO with both Ag and Ti S/D electrodes were calculated by the following approximations:[16,17]

$$L_T = \frac{R_{S/D}}{r_{Ceff}}, \quad (5)$$

$$r_{Ceff} = WL_T^2 r_{ch} = \frac{WR_{S/D}^2}{r_{ch}}, \quad (6)$$

$$R_C = R_{SD}L_T W. \quad (7)$$

Both r_{Ceff} and $R_{S/D}$ values for *a*-IGZO TFTs with reference Ag and Ti S/D electrodes dramatically decreased with increased V_{GS} within a measured range. However, the *a*-IGZO TFT with Ti S/D electrodes exhibited lower Rc, r_{Ceff}, and $R_{S/D}$ values ($1.65 \times 10^{-2}\ \Omega\ cm^2$, $8.71 \times 10^{-3}\ \Omega\ cm^2$, and $507\ \Omega$) than the *a*-IGZO TFT with reference Ag S/D electrodes ($4.57 \times 10^{-2}\,\Omega\,cm^2$, $2.29 \times 10^{-2}\,\Omega\,cm^2$, and $858\,\Omega$) at $V_{GS} = 24$ V, in spite of the high resistivity of Ti metal. Furthermore, the *a*-IGZO TFT with Ti S/D electrodes had smaller L_T values than the TFT with Ag S/D electrodes, regardless of V_{GS}. It is well known that L_T increases with the thickness of the semiconducting layer, bulk density-of-states, and S/D contact resistance.[20] The r_{Ceff} values were also affected by S/D contact resistivity and by the bulk resistivity of *a*-IGZO. With identical *a*-IGZO channel layer and deposition processes, L_T and r_{Ceff} values were negligibly influenced by thickness, bulk density-of-states, and bulk resistivity. This can be attributed to reduced contact resistivity between Ti and *a*-IGZO caused by the formation of an interfacial layer, even for *a*-IGZO with low carrier concentration. In *a*-Si:H TFT system, larger R_C is known to be the reason of applied drain voltage drop, leading to a reduced filed-effect mobility.

In summary, we studied the effects of Ti contact on the properties of *a*-IGZO semiconducting layers and correlated the effects with electrical contribution to TFT devices. The formation of a TiO_x interfacial layer between Ti and *a*-IGZO was found to have led to the formation of an oxygen deficient region in the IGZO contact region. The oxygen deficient region caused TFTs with Ti S/D contact to show a negative shift in V_T of 3.46 V and relative high μ_{SAT} values of 8.48 cm^2/Vs. In addition, we observed relatively low r_{Ceff}, $R_{S/D}$, and L_T values for *a*-IGZO TFTs with Ti S/D electrodes because a low contact resistivity (R_C) originated from increased carrier concentration at the Ti/*a*-IGZO interface. Based on HRTEM and XPS analyses, we suggested a possible mechanism to explain Ti contact on the *a*-IGZO channel layer with low carrier concentration.

This work was mainly supported by the Samsung Mobile Displays Research Center Program and was partially supported by the Industrial Core Technology Development Programs of the Korea Ministry of Knowledge Economy (Grant No. 10033573).

[1]K. Nomura, H. Ohta, K. Ueda, T. Kamiya, M. Hirano, and H. Hideo, Science **300**, 1269 (2003).
[2]A. Takagi, T. Kamiya, M. Hirano, and H. Hosono, Nature (London) **432**, 488 (2004).
[3]H. Yabuta, M. Sano, K. Abe, T. Aiba, T. Den, H. Kumomi, K. Nomura, T. Kamiya, and H. Hosono, Appl. Phys. Lett. **89**, 112123 (2006).
[4]B. D. Ahn, H. S. Shin, H. J. Kim, J.-S. Park, and J. K. Jeong, Appl. Phys. Lett. **93**, 203506 (2008).
[5]K.-H. Choi, H.-W. Koo, T. W. Kim, and H.-K. Kim, Appl. Phys. Lett. **100**, 263505 (2012).
[6]W.-S. Kim, Y.-K. Moon, S. Lee, B.-W. Kang, T.-S. Kwon, K.-T. Kim, and J.-W. Park, Phys. Status Solidi (RLL) **3**, 239 (2009).
[7]S. Kim, K.-K. Kim, and H. Kim, Appl. Phys. Lett. **101**, 033506 (2012).
[8]J.-R. Yim, S.-Y. Jung, H.-W. Yeon, J.-Y. Kwon, Y.-J. Lee, J.-H. Lee, and Y.-C. Joo, Jpn. J. Appl. Phys., Part 1 **51**, 011401 (2012).
[9]P. Barquinha, A. M. Vilà, G. Gonçalves, L. Pereira, R. Martins, J. R. Morante, and E. Fortunato, IEEE Trans. Electron Devices **55**, 954 (2008).
[10]P. Barquinha, A. M. Vilà, G. Gonçalves, L. Pereira, R. Martins, J. Morante, and E. Fortunato, Phys. Status Solidi A **205**, 1905 (2008).
[11]H. Kim, K.-K. Kim, S.-N. Lee, J.-H. Ryou, and R. D. Dupuis, Appl. Phys. Lett. **98**, 112107 (2011).
[12]J.-S. Park, J. K. Jeong, Y.-G. Mo, H. D. Kim, and C.-J. Kim, Appl. Phys. Lett. **93**, 033513 (2008).
[13]T. T. Trinh, V. D. Nguyen, J. Ryu, K. Jang, W. Lee, W. Back, J. Raja, and J. Yi, Semicond. Sci. Technol. **26**, 085012 (2011).
[14]*Handbook of X-Ray Photoelectron Spectroscopy*, edited by J. F. Moulder, W. F. Stickle, P. E. Sobol, K. D. Bomben and J. Chastain (Perkin-Elmer, Eden Prairie, 1992), p. 72.
[15]H.-Ki. Kim, S.-H. Han, T.-Y. Seong, and W.-K. Choi, Appl. Phys. Lett. **77**, 1647 (2000).
[16]C. R. Kagan and P. Andry, *Thin-Film Transistors* (Marcel Dekker, Inc., 2003).
[17]J. Park, C. Kim, S. Kim, I. Song, S. Kim, D. Kang, H. Lim, H. Yin, R. Jung, E. Lee, J. Lee, K.-W. Kwon, and Y. Park, IEEE Electron Device Lett. **29**, 879 (2008).
[18]S. Lee, J.-H. Park, K. Jeon, S. Kim, Y. Jeon, D. H. Kim, D. M. Kim, J. C. Park, and C. J. Kim, Appl. Phys. Lett. **96**, 113506 (2010).
[19]D. K. Schroder, *Semiconductor Materials and Device Characterization*, 3rd ed. (John Wiley & Sons, Inc., 2005), p. 130.
[20]S. Martin, C.-S. Chiang, J.-Y. Nahm, T. Li, J. Kanicki, and Y. Ugai, Jpn, J. Appl. Phys., Part 1 **40**, 530 (2001).